IEEE Open Journal of
Power Electronics

Received 14 August 2021; revised 10 September 2021; accepted 20 September 2021. Date of publication 24 September 2021; date of current version 15 October 2021. The review of this article was arranged by Associate Editor Jin Ye.

*Digital Object Identifier 10.1109/OJPEL.2021.3115404*

# Open Phase Fault Tolerant Control of Multi Three Phase Machines

**JAYAKRISHNAN HARIKUMARAN [1], GIAMPAOLO BUTICCHI [1,2] (Senior Member, IEEE), MICHAEL GALEA [1,2] (Senior Member, IEEE), AND PATRICK WHEELER [1] (Fellow, IEEE)**

[1]Department of Power Electronics Machines and Control (PEMC) Research Group, University of Nottingham, Nottingham NG72RD, U.K.
[2]Key Laboratory of More Electric Aircraft Technology of Zhejiang Province, University of Nottingham Ningbo China, Ningbo 315100, China

CORRESPONDING AUTHOR: GIAMPAOLO BUTICCHI (e-mail: buticchi@ieee.org).

This work was supported by INNOVATIVE Doctoral Program, which is funded through Marie Curie Initial Training Networks Action under Grant 665468. This project also received funding from the Clean Sky 2 Joint Undertaking under the European Union's Horizon 2020 research and innovation programme under Grant 807081.

**ABSTRACT** Drive system availability is critical in aerospace applications. Multi three phase machines are a known solution to provide redundancy and fault tolerance capability. Control of multi three phase machines is typically implemented in DQ domain or VSD domain. An alternate control approach is per phase current control using proportional resonant controllers in ABC domain. In this work, ABC domain current controllers are utilized to demonstrate key advantages in high reliability applications - fault reconfigurability with minimal controller modifications and ability to control multiple harmonic components. ABC domain control structure enables seamless transition from healthy mode to fault mode with only algebraic operations at the controller output unlike DQ/VSD domains. Furthermore, single-phase operating mode in ABC domain provides an additional fault mode for emergency operation which is unavailable in DQ/VSD control domains. The Fault mode operation under open circuit fault of one phase in each winding set is demonstrated. Simulation and experimental results validate the normal and fault condition operation of the proposed control method.

**INDEX TERMS** Multi three phase machine, more electric aircraft, fault tolerance, multi level converter.

## NOMENCLATURE

| | |
|---|---|
| AEA | All electric aircraft |
| EMF | Electromotive Force |
| IPM | Interior Permanent Magnet |
| MCU | Micro controller unit |
| MEA | More electric aircraft |
| MMF | Magneto-Motive Force |
| NPC | Neutral point clamped |
| PCB | Printed circuit board |
| SOGI | Second Order Generalized Integrator |
| SPM | Surface Permanent Magnet |
| VSD | Vector Space Decomposition |
| 3L-NPC | Three Level Neutral Point Clamped |

## I. INTRODUCTION

Electrical systems are being increasingly adopted is aviation sector as a substitute for mechanical counter-parts. On-board electrical generation has touched 1 MVA and is on the rise [1]. The trend of electrification is driven by multiple requirements - societal demand for emission reduction and higher performance, efficiency and simplified maintenance of electrical systems. Recently MEA and AEA concepts are being considered for introduction of electrical propulsion. The backbone for electrical propulsion is the electric drive consisting of-electric motors/generators, power electronic converters, control platform and sensors [2].

In order to meet aerospace fault tolerance requirements [3], redundancy and fault tolerance must be built into the propulsion system. Fault tolerance in applications requiring process continuity, for instance process industry, multi-phase machines and multi three phase systems have been gaining increasing popularity [4]. The key advantage of a multi three phase machine in comparison to a conventional 3 phase machine is the ability to generate a rotating MMF

and consequently, a smooth torque after failure of one or more phases [5], [6]. Hence multi-phase machines are being considered for future MEA/AEA propulsion applications.

The fundamental system equations in terms of flux linkages for a multi-phase machine was shown in [7]. Typically, a transformation is applied - Clarke transformation in the case of three phase machine and VSD transformation is performed for multi-phase machines and current control is carried out in the transformed space.

Prior literature has extensively studied the two methods of multi three phase machine control - DQ control, where each three phase set is considered independently ignoring mutual coupling between winding sets [8] and VSD based control [9], [10]. The mismatch in torque estimation and reduction in control performance of independent DQ control when inter winding coupling is not accounted for is shown in [11]. A comparison between VSD and DQ control and the conditions under which the two are equivalent is shown in [12]. DQ control is chosen when independent control of 3 phase winding sets is a requirement. This feature is important from a safety certification point of view for high reliability applications, where a single point failure (controller in VSD method) could lead to failure of the whole system. The work in [13] provides a model for independent DQ control based on some approximations. The model is similar to the one derived from VSD transformation. Another approach was proposed by [14], a distributed control scheme based on VSD analysis. Both the above approaches provide the ability to perform independent current control of each winding set. The above methods do not propose a fault mode reconfiguration mechanism other than disabling the faulty winding set.

Fault tolerance method for a multi three phase machine with common neutral was proposed in [15]. The current references of remaining healthy phases are modified to generate a rotating MMF. In [16], fault mode control of a dual three phase machine with two isolated neutrals is presented. The current controller is reconfigured such that the machine is operated with two single-phase winding sets operating in quadrature to each other. This approach is very interesting and a mathematical method of estimating the fault current references is presented in this work.

In this paper, control of a dual three phase machine using PR controllers is implemented. It would be shown that, controller implementation in ABC domain is comparable in computational complexity with respect to DQ or VSD methods. The key contributions of this paper are the fault mode controller reconfiguration and current reference generation to maximize torque in fault mode. The controller in ABC domain is easily reconfigurable for fault mode control. Single open phase fault and dual open phase fault operation is presented and experimentally validated.

The paper is organized as follows. Section II presents the equivalent per phase model of an asymmetric dual three phase machine. Section III describes the PR controller structure in the healthy mode as well as the fault mode reconfiguration of the controllers. Section IV presents the tuning of the current controllers and the simulated response of the system under study. Finally, experimental validation of the proposed fault mode operation is presented in Section V and paper is concluded in Section VI.

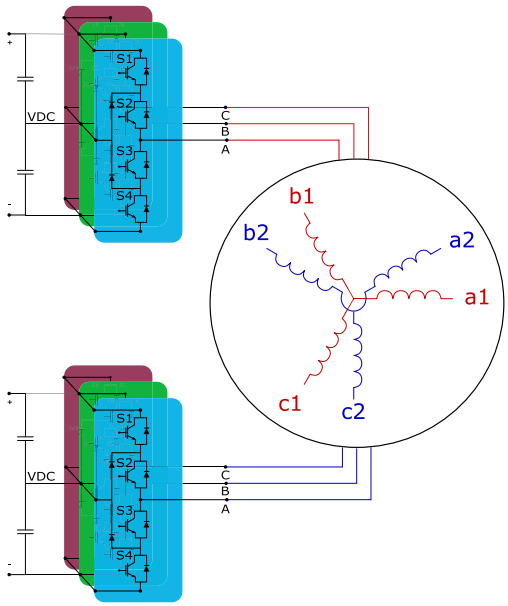


**FIGURE 1.** 6 phase machine with isolated neutrals.

## II. MULTI 3 PHASE DRIVE SYSTEM

An asymmetrical six-phase machine with isolated neutrals is analysed in this study. The analysis can be easily extended to higher winding set configurations. The machine drive system is showin in Fig. 1. Each three-phase set is fed by a 3L-NPC converter.

### A. MACHINE MODELLING AND CONTROL

The equivalent per phase model of the machine is derived in this section. The phase progression angles are shown with the reference axis aligned with phase a1.

$$\begin{aligned} &= \left[0 \ \tfrac{\pi}{6} \ \tfrac{2\pi}{3} \ \tfrac{5\pi}{6} \ \tfrac{4\pi}{3} \ \tfrac{9\pi}{6}\right] \\ &= \left[\theta_{a1} \ \theta_{a2} \ \theta_{b1} \ \theta_{b2} \ \theta_{c1} \ \theta_{c2}\right] \end{aligned} \tag{1}$$

The stator voltage equation matrix with permanent magnet flux $\lambda_m$ can be expressed in most general form as

$$\begin{aligned} [V_s] &= [R_s]\cdot[i_s] + p\cdot[\lambda_s] \\ &= [R_s]\cdot[i_s] + p([L_{ss}][i_s] + \lambda_m cos[\omega t - \theta_x]) \end{aligned} \tag{2}$$

where, the voltage and current vectors are defined as

$$[V_s] = \begin{bmatrix} V_{a1} \\ V_{a2} \\ V_{b1} \\ V_{b2} \\ V_{c1} \\ V_{c2} \end{bmatrix} \quad [i_s] = \begin{bmatrix} i_{a1} \\ i_{a2} \\ i_{b1} \\ i_{b2} \\ i_{c1} \\ i_{c2} \end{bmatrix}$$

The resistance and inductance matrices in (2) are defined as follows.

$$R_s = r_s \begin{bmatrix} 1 & 0 & \cdots & 0 \\ 0 & 1 & \cdots & 0 \\ \vdots & \vdots & \ddots & \vdots \\ 0 & 0 & \cdots & 1 \end{bmatrix} \tag{3}$$

$$L_{ss} = L_{ls} \begin{bmatrix} 1 & 0 & \cdots & 0 \\ 0 & 1 & \cdots & 0 \\ \vdots & \vdots & \ddots & \vdots \\ 0 & 0 & \cdots & 1 \end{bmatrix} + L_A \begin{bmatrix} cos[\Theta_{a1}] \\ cos[\Theta_{a2}] \\ cos[\Theta_{b1}] \\ cos[\Theta_{b2}] \\ cos[\Theta_{c1}] \\ cos[\Theta_{c2}] \end{bmatrix} - L_B \begin{bmatrix} cos[2(\omega t - \Theta L_{Ba1})] \\ cos[2(\omega t - \Theta L_{Ba2})] \\ cos[2(\omega t - \Theta L_{Bb1})] \\ cos[2(\omega t - \Theta L_{Bb2})] \\ cos[2(\omega t - \Theta L_{Bc1})] \\ cos[2(\omega t - \Theta L_{Bc2})] \end{bmatrix} \tag{4}$$

$L_{ls}, L_A, L_B$ is the stator leakage inductance, average value of magnetizing inductance and variation amplitude of magnetizing inductance respectively.

The angle matrices $[\Theta_{a1}], [\Theta_{a2}] \ldots$ represent the relative angle difference between any particular $phase_{xn}$ with other phases. They are given by

$$[\Theta_{xn}] = [\Theta - \theta_x]$$

The $[\Theta L_B]$ matrix of each phase accounts for variation in magnetizing inductance for different phases. It is computed as half of the angle between the phases x and y added to the absolute angle from reference of phase x. For instance, $\theta L_{Ba2-a3} = \theta_{a2} + \frac{\theta_{a3} - \theta_{a2}}{2}$. The $[\Theta L_B]$ matrix for phases $a1$ and $a2$ are provided for reference.

$$= \begin{bmatrix} 0 & \frac{\pi}{12} & \frac{4\pi}{12} & \frac{5\pi}{12} & \frac{8\pi}{12} & \frac{9\pi}{12} \end{bmatrix}$$

$$[\Theta L_{Ba2}] = \begin{bmatrix} \frac{\pi}{12} & \frac{2\pi}{12} & \frac{5\pi}{12} & \frac{6\pi}{12} & \frac{9\pi}{12} & \frac{10\pi}{12} \end{bmatrix}$$

Direct and quadrature inductance values, $L_d, L_q$ in case of a synchronous reluctance machine are related to $L_{ls}, L_A, L_B$ as follows

$$L_d = L_{ls} + \frac{3N}{2}(L_A - L_B) \tag{5}$$

$$L_q = L_{ls} + \frac{3N}{2}(L_A + L_B) \tag{6}$$

(2) to (4) is a complete representation of the asymmetrical 6 phase machine. Typical control approaches perform a Clarke transform or a VSD transformation to the machine model to derive a rotating reference frame equivalent model of the system. In order to further develop the machine model in ABC domain, the following conditions which apply to synchronous reluctance machine is considered. In a machine without inherent asymmetries only the fundamental harmonic is useful for torque generation. In order to generate a smooth mechanical

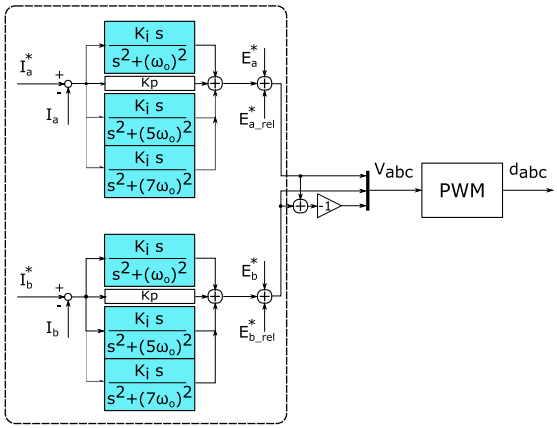


**FIGURE 2.** PR control structure per inverter.

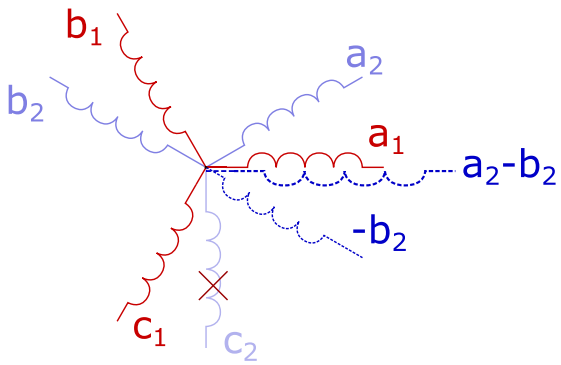


**FIGURE 3.** Fault mode machine.

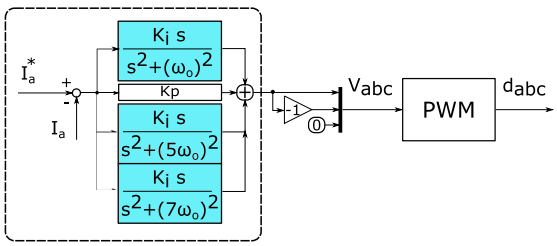


**FIGURE 4.** Single-phase open fault mode control structure.

torque, the stator currents must sum up to generate a rotating MMF. Hence the current references in a 6 phase machine can be expressed as

$$[i_s] = \begin{bmatrix} K_1 \cdot I \cdot cos[\omega t - \theta_{a1} + \phi] \\ K_2 \cdot I \cdot cos[\omega t - \theta_{a2} + \phi] \\ K_1 \cdot I \cdot cos[\omega t - \theta_{b1} + \phi] \\ K_2 \cdot I \cdot cos[\omega t - \theta_{b2} + \phi] \\ K_1 \cdot I \cdot cos[\omega t - \theta_{c1} + \phi] \\ K_2 \cdot I \cdot cos[\omega t - \theta_{c2} + \phi] \end{bmatrix} \tag{7}$$

Applying (7) in (2), the voltage equation per phase can be written as

$$V_x = \Big(r_s + pL_{ls}\Big) i_x + pL_A \sum_{y=1}^{3N} i_y cos(\theta_y - \theta_x)$$

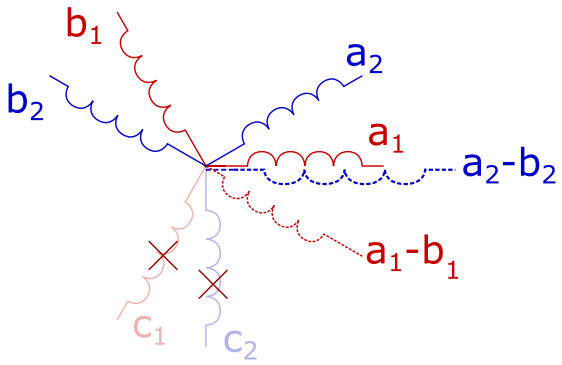


**FIGURE 5.** Double fault mode machine.

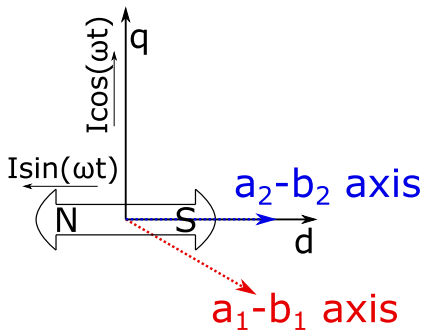


**FIGURE 6.** Rotating flux generated with two single-phase windings.

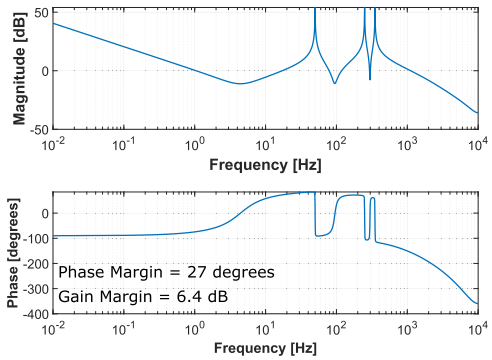


**FIGURE 7.** Bode plot of PIR controller tuned at fundamental frequency - 100Hz.

$$- pL_B \sum_{y=1}^{3N} i_y cos(2\omega t - \theta_x - \theta_y) + p\lambda_m cos(\omega t - \theta_x) \tag{8}$$

$$i_x = K_w I cos(\omega t - \theta_x + \phi) \tag{9}$$

$$V_x = r_s \cdot i_x + p\left(L_{ls} + \frac{3}{2} L_A \sum_{w=1}^{N} \frac{K_w}{K_x}\right) i_x - p\left(\frac{3}{2} L_B I cos(\omega t - \theta_x - \phi) \sum_{w=1}^{N} K_w\right) - \omega\lambda_m sin(\omega t - \theta_x) \tag{10}$$

As can be noted, the sum of current sharing coefficients equal number of winding sets, the equations can be written in a form which is identical in form to the VSD equation.

$$V_x = r_s \cdot i_x + p\left(L_{ls} + \frac{3N}{2 \cdot K_x} L_A\right) i_x - p\left(\frac{3N}{2} L_B I cos(\omega t - \theta_x - \phi)\right) - \omega\lambda_m sin(\omega t - \theta_x) \tag{11}$$

The first two terms in (11) account for machine flux dynamics represented in a per phase basis. The third term and fourth terms account for reluctance generated back emf, denoted as $E_{xrel}$, and permanent magnet flux generated back emf, denoted as $E_x$ respectively. The reluctance generated back emf cannot be ignored in IPM machines. Reluctance generated back emf has a phase shift of $-2\phi$ with respect to the applied current. The phase voltage equation illustrates the inter-winding set interaction. System state dependency on $K_x$, should be accounted for in the current controller.

The system model is very similar to the Clarke or VSD transformed system equations with only the reluctance variation accounted for as a separate potential term. This result in the present form is obtained due to the spatial and time dependence of the phase currents. It should be mentioned that this approach can be generalized to any spatial distribution of coils and current references. Any current distribution in a three-phase winding set with isolated neutral can be expressed as a positive and negative sequence combination.

Net mechanical torque developed is easily calculated by summing the power transferred by each phase. In healthy mode, the system torque is given by (12). This expression is in fact identical to the equations derived in DQ or VSD domain. The torque expression can be used to setup the speed/flux control loop in an identical manner to the DQ/VSD domains. Instead of providing $I_d$ and $I_q$ setpoints to regulate torque and flux, phase current amplitude and phase angle, $\phi$ are the setpoints required in ABC domain. Hence the calculation complexity or lookup tables necessary for the outer speed/flux controllers are identical compared to the conventional synchronous reference frame approaches.

$$T_m = \frac{3N}{2} \frac{p}{2} \left(\lambda_m I sin(\phi) - \frac{3N}{2} L_B I^2 sin(2\phi)\right) \tag{12}$$

## III. ABC DOMAIN CONTROL STRUCTURE

The detailed control structure for a single converter in normal operation is shown below. Only 2 PR controllers are necessary per inverter and control signal for third phase is obtained by an arithmetic relation. Multiple resonant terms can be added within the controller bandwidth to eliminate higher order harmonics.

The PR controller structure is easily reconfigurable for fault conditions as shown in Section III-A.

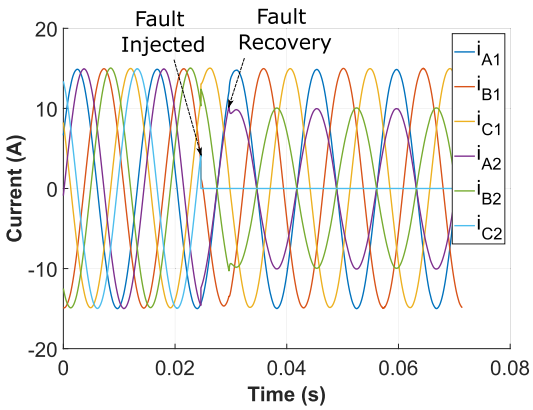


(a) Simulated phase currents with phase C2 open

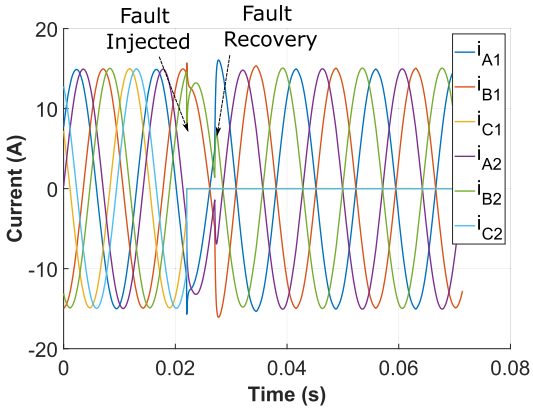


(b) Simulated phase currents with phases C1 and C2 open

**FIGURE 8.** Simulated phase faults.

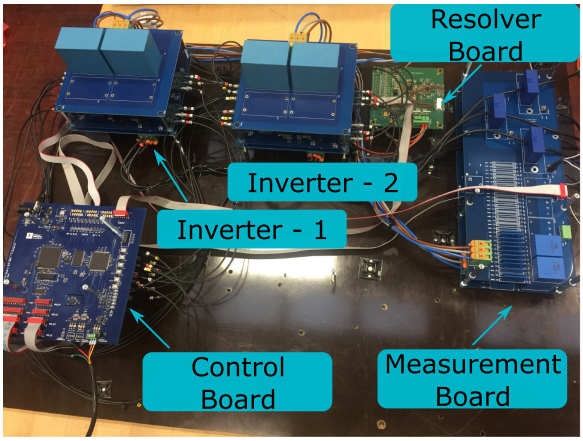


(a) 3LNPC Drive Prototype

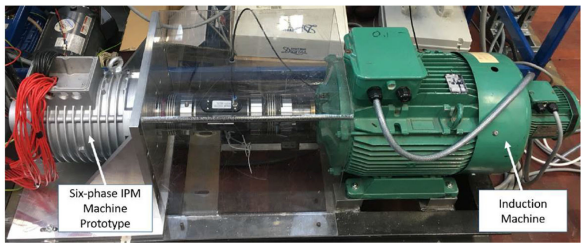


(b) IPM Machine Setup

**FIGURE 9.** NPC based Drive Setup.

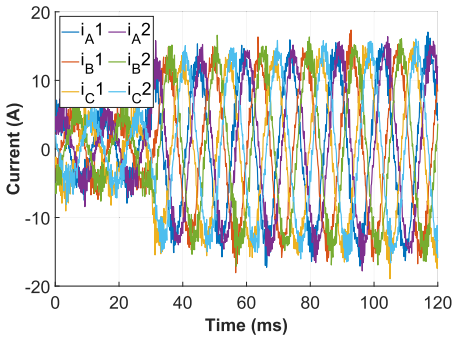


**FIGURE 10.** Transient response of healthy drive system.

### *A. DOMINANT FAULT MODES OF DRIVE SYSTEMS*

The dominant fault modes in industrial drives have been described and quantified in [17]. Approximately 40% of the faults are attributed to power circuits with a large portion caused by power semiconductors. Semiconductor faults are either open circuit fault or short circuit fault. According to [18], the predominant failure mode in IGBTs is open circuit fault. The above is valid in the case of wire bound IGBT modules while for press-pack modules, short circuit failure mode is more common. In the case of 3L-NPC converter, fault modes of inner and outer IGBTs presents different options for fault reconfiguration. Practically, inner switch fault prevents fault reconfiguration for motor drive applications, even though it can be mitigated for grid connected applications [19]. Short circuit fault of the outer IGBT can be potentially destructive for the inner IGBT as the entire DC link voltage would be applied across it. Fault reconfiguration is a possibility under open fault of outer IGBTs.

In the case of multi three phase drive systems with 3L-NPC converters, the fault reconfiguration option is to operate the faulty three-phase winding set in single-phase mode. Two different fault modes are studied in this work - open phase fault in phase C2 alone and open phase faults in phases C2 and C1 of a dual three phase machine.

#### 1) SINGLE OPEN PHASE FAULT

In the previous section, fault reconfiguration options for 3L-NPC based drive systems were described. Operating the

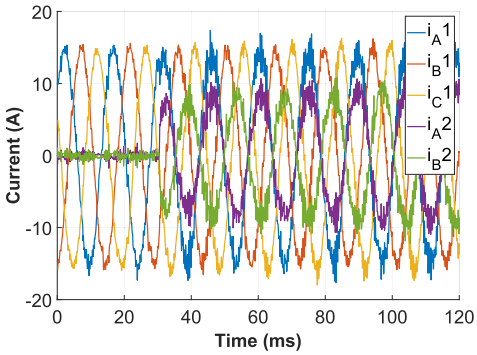


(a) Phase currents with phase C2 open

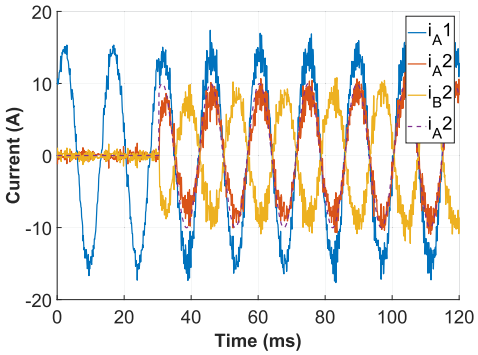


(b) Reference tracking in single-phase fault

**FIGURE 11.** Single-phase open fault mode current control.

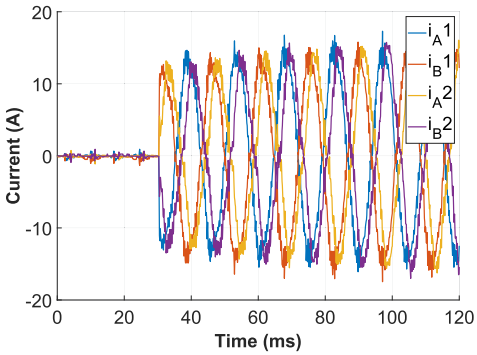


(a) Phase currents with phases C1 and C2 open

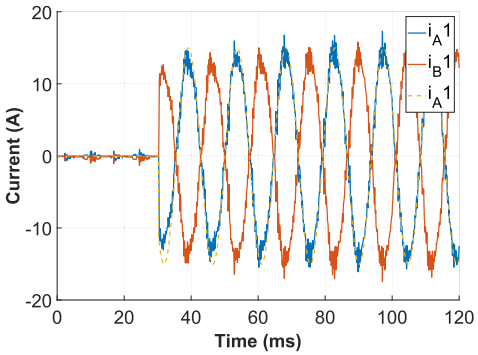


(b) Reference tracking in dual phase fault

**FIGURE 12.** Dual phase open fault mode control.

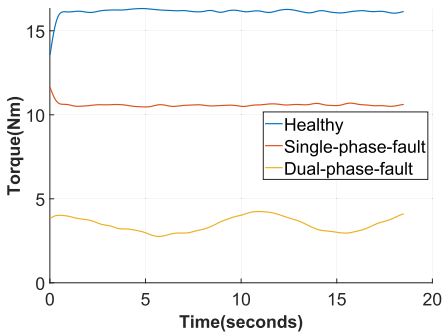


**FIGURE 13.** Torque comparison across modes.

healthy phases as a single-phase winding set is considered as the fault mode operation in this work.

As one phase is open, the two remaining windings carry the same current and behave as a single winding set (Fig. 3).

$$i_{a2} = K_{S2} I cos(\omega t + \phi_{S2}) \tag{13a}$$

$$i_{b2} = -K_{S2} I cos(\omega t + \phi_{S2}) \tag{13b}$$

The system equations for the healthy winding sets and the faulty set in single-phase operation is derived for development of controllers. The individual phase voltages after fault can be derived from (8). The single-phase set voltage equation takes the form of a line to line voltage equation.

$$\begin{aligned} V_{a_2 b_2} = {} & 2r_s \cdot i_{a2} + p\left(2L_{ls} + 3L_A\right) i_{a2} \\ & + p\left(\sqrt{3}\frac{3(N-1)}{2} L_A\right) I cos(\omega t - \theta_{a2} + \frac{\pi}{6} + \phi) \\ & + p\left(3L_B i_{a2} \cos\left(2\omega t - 2\theta_{a2} - \frac{2\pi}{3}\right)\right) \\ & - p\left(\sqrt{3}\frac{3(N-1)}{2} L_B I cos(\omega t - \theta_{a2} + \frac{\pi}{6} - \phi)\right) \\ & - \sqrt{3}\omega\lambda_m sin(\omega t - \theta_{a2} + \frac{\pi}{6}) \end{aligned} \tag{14}$$

The healthy winding set voltage equations are also impacted by the faulty winding.

$$\begin{aligned} V_x = {} & r_s \cdot i_x + p\left(L_{ls} + \frac{3}{2} L_A \sum_{w=1}^{N-1} \frac{K_w}{K_x}\right) i_x \\ & + p\left(\sqrt{3} L_A i_{a2}\right) cos(\theta_x - \theta_{a2} + \frac{\pi}{6}) \\ & - p\left(\frac{3}{2} L_B I cos(\omega t - \theta_x - \phi) \sum_{w=1}^{N-1} K_w\right) \end{aligned}$$

$$- p\left(\sqrt{3}L_B i_{a2} cos(2\omega t - \theta_x - \theta_{a2} + \frac{\pi}{6})\right)$$
$$- \omega\lambda_m sin(\omega t - \theta_x) \quad (15)$$

The loss of three phase symmetry leads to harmonics in phase voltages. The healthy winding set continues to generate a rotating MMF. The faulty winding set in single-phase mode can add an additional torque component albeit a pulsating torque contribution.

From the machine stator voltage equations, it can be observed that the machine reduces to a four winding set system with a new effective winding set a2-b2. The effective winding set in case of the six-phase machine is aligned with phase a1 given by vector summation of flux generated by the currents through phase a2 and b2. Hence the current reference of the single-phase winding must be set with a phase shift to reflect the effective orientation of the fictitious winding set a2-b2 as shown in (16). The magnetizing current and inter winding magnetizing inductance due to the single-phase set is scaled by a factor of $\sqrt{3}$ for the fundamental component.

$$\phi_{S2} = -\theta_{a2} + \frac{\pi}{6} + \phi \quad (16)$$

The control structure in the single-phase case is very similar to the healthy mode as seen in Fig. 4. The faulty phase is left uncontrolled while only a single PR controller is required to control the single-phase set.

The net torque of the 4 winding set operation can be derived as (17).

$$T_{3ph} = \frac{3(N-1)}{2}\frac{p}{2}\left(\lambda_m I sin(\phi) - \frac{3(N-1)}{2}L_B I^2 sin(2\phi)\right. \quad (17a)$$
$$\left. - \frac{\sqrt{3}}{2}L_B K_{S2} I^2 sin(2\phi)\right)$$
$$T_{sph} = \frac{\sqrt{3}}{2}\frac{p}{2}\left(\lambda_m K_{S2} I sin(\phi) - \frac{3(N-1)}{2}L_B K_{S2} I^2 sin(2\phi)\right. \quad (17b)$$
$$\left. - \frac{\sqrt{3}}{2}L_B K_{S2}^2 I^2 sin(2\phi)\right)$$
$$T_{4ph} = T_{3ph} + T_{sph} \quad (18)$$

### 2) DUAL SINGLE OPEN PHASE FAULT

A more severe fault condition is when one phase in each winding set suffers from open faults. The machine effectively reduces to a dual winding set machine. The winding set distribution including fictitious single-phase systems is shown in Fig. 5.

$$\theta_{a1-b1} = \theta_{S1} = -\frac{\pi}{6} \quad (19a)$$
$$\theta_{a2-b2} = \theta_{S2} = 0 \quad (19b)$$

The machine stator voltages can be derived as before starting with (8).

$$V_{a_1 b_1} = 2r_s \cdot i_{a1} + p\left(2L_{ls} + 3L_A\right)i_{a1}$$
$$+ p\left(3L_A\right)i_{a2}\cos(\theta_{a2} - \theta_{a1})$$
$$+ p\left(3L_B i_{a1}\cos\left(2\omega t - 2\theta_{a1} - \frac{2\pi}{3}\right)\right)$$
$$+ p\left(3L_B i_{a2}\cos\left(2\omega t - \theta_{a1} - \theta_{a2} - \frac{2\pi}{3}\right)\right)$$
$$- \sqrt{3}\omega\lambda_m \sin(\omega t - \theta_{a1} + \frac{\pi}{6}) \quad (20)$$

In the case of dual single-phase fault, rotating MMF is not present from the healthy winding set. Hence the single-phase currents must generate a rotating MMF to develop torque in the machine. A rotating MMF condition is satisfied by the presence of orthogonal current/flux components given by (21).

$$I cos(\omega t) = -i_{a1} sin(\theta_{S1}) - i_{a2} sin(\theta_{S2})$$
$$-I sin(\omega t) = i_{a1} cos(\theta_{S1}) + i_{a2} cos(\theta_{S2}) \quad (21)$$

The above equations are derived by fixing the rotating stator flux at an angle 90°with respect to the rotor without accounting for reluctance torque. The graphical visualization is shown in Fig. 6.

The general equation in (21) can be solved for the particular situation at hand by applying the restrictions from (19).

$$I_{a1} = 2 \cdot I$$
$$\phi_{S1} = -\pi$$
$$I_{a2} = 2 \cdot I$$
$$\phi_{S2} = \frac{\pi}{6} \quad (22)$$

The torque contribution from each single-phase set can be calculated as shown in (23).

$$T_{S1} = \frac{\sqrt{3}}{2}\frac{p}{2}\left(\lambda_m I_{a1}\sin\left(\frac{\pi}{6}\right)\right)$$
$$T_{S2} = \frac{\sqrt{3}}{2}\frac{p}{2}\left(\lambda_m I_{a1}\sin\left(\frac{\pi}{6}\right)\right) \quad (23)$$

The controller structure is identical to the single open phase fault condition as shown in Fig. 4. Both winding sets are operated as single-phase winding sets with the current phase angles derived in (22). A comparison is made to the fault mode control proposed in [16]. The above referred method requires a controller reconfiguration while not able to provide a single-phase fault mode operation. The machine control is directly transitioned to the presented dual phase fault operation. The potential for higher torque is lost by operating in dual phase fault mode. Another key advantage for the proposed method in comparison to the literature method is lack of controller modification which is required in the latter.

**TABLE 1. Converter/Machine/PIR Tuning Parameters**

| | |
|---|---|
| **DC link Voltage** | 270V |
| **DC link Capacitance** | 101.1uF |
| **Machine pole pairs** | 4 |
| **Machine operating speed** | 1050 rpm |
| $\lambda_m$ | 0.0923 V/rad/s |
| **Converter Switching Frequency** | 20 kHz |
| **Datalogger Sampling Frequency** | 10 kHz |
| **Torque Datalogger Sampling Frequency** | 100 Hz |
| $K_P$ | 0.42 |
| $K_R$ | 750 |
| $K_I$ | 10 |
| $K_{damp}$ | 0.05 |

## IV. SIMULATIONS OF DUAL THREE PHASE DRIVE

A simulation model for a dual three phase machine was developed using PLECS blockset in Simulink to verify the current controller performance of the 3L-NPC converters.

### A. TUNING OF THE CURRENT CONTROLLER

The machine model is simplified to a RL load with a back emf term to tune the PR controller. The discrete plant transfer function including the effect of Zero order hold and computational delay is given by (24)

$$G_{PL}(z) = \frac{z^{-2}}{R}\frac{1-\rho^{-1}}{1-z^{-1}\rho^{-1}} \tag{24}$$

where $\rho = e^{R\cdot T_s/L}$

The ideal PR controller structure is shown in Fig. 2. A damping term is added to the resonant term for practical implementation. In the case of drives, the resonant terms do not provide high gain at zero speed. Hence an integrator is added to the controller to improve start-up performance. The full control structure in s-domain is given by (25)

$$G_{PIR}(s) = K_P + \frac{K_I}{s} + K_R \sum_{h=1}^{h_{max}} \frac{k_{damp}(h\omega)s}{s^2 + k_{damp}(h\omega)s + (h\omega)^2} \tag{25}$$

The integrator term is discretized using the tustin method while the resonant term is implemented using the SOGI method [20]. The SOGI consists of two integrators and the method for their discretization influences the frequency response. The forward integrator is discretised using forward Euler method and the feedback integrator using backward Euler method according to [21]. Tuning of the PR controller is performed to achieve a crossover frequency of 1kHz for the current controller. $K_R$ is chosen to get a high gain at the frequencies to track. The tuning procedure is as described in [22]. The PR parameters are summarized in Table 1.

The open loop bode plot of the Plant and the PIR controller is plotted in Fig. 7. It should be noted that the margins obtained for the controller accounts for the discretization effects.

#### 1) DC LINK BALANCING OF NPC CONVERTERS

DC link balancing is essential for NPC operation. A modified balancing method is implemented based on [23] and [24]. During fault operation, the converters are operated in single-phase mode and the zero sequence injection is not available for balancing.

### B. SIMULATED RESPONSES OF THE DRIVE SYSTEM

The simulated fault responses of the drive system are presented here. The transition to single-phase fault as well as dual phase fault are simulated. In simulation fault injection is achieved by switching is a high value series resistance. In experiments, the fault injection is achieved by turning gate signals off for one of the phases. The fault recovery behaviour in experiments is to trip and restart even though a seamless transfer is possible. The trip restart is chosen as the phase reference would be sub-optimal for maximizing torque and it could potentially lead to controller instability as the remaining phase controllers are in contention to regulate the phase current. Minimal disruption is still achieved as the demonstrated by the transient response of the faulty current controllers. A fault detection time of 5ms is simulated. The controllers seamlessly transition to the fault mode operation. In practical implementation, the fault transient may trip the converters. The recovery from fault state is shown in the experimental results. The fault responses shown in Fig. 8 are simulated at the same conditions as the experimental setup as summarizedd in Table 1.

## V. EXPERIMENTAL SETUP

The experimental validation is carried out on a dual neutral 6 phase IPM machine. 3L-NPC converter prototypes developed based on "FS3L30R07W2H3F_B11" power module from Infineon rated at 650V and 30A are used as the drive converters. The control code is run on a C2000 family floating point DSP (F28377D) clocked at 200MHz. The controller for each three-phase set is run independent from each other. The experimental setup is shown in Fig. 9.

Key parameters of interest of the experimental setup are summarized in table below:

Step response of the drive system in healthy condition to verify tuning is shown in Fig. 10.

The waveforms when phase sets are healthy are not included for brevity. The single-phase open fault is considered first. As the fault develops, one phase set goes offline. The healthy winding set continues to operate and provides half the torque to the machine. The reconfiguration in control code for the faulty winding set is straightforward as shown in Fig. 4.

The current waveforms as well as the reference tracking is shown in Fig. 11. The healthy winding set current reference is set to 15A while the single-phase set is programmed with a current reference of 10A.

Dual phase fault where phase C1 and phase C2 suffers open phase fault is shown in Fig. 12. The current reference for each single-phase set is set to 15A.

**TABLE 2. Torque Comparison**

| Operating mode | Predicted Torque | Measured Torque |
|---|---|---|
| Healthy - $I_{Ph}$ - 15A | 16.61 Nm | 16.3 Nm |
| single-phase fault<br>Healthy $I_{Ph}$ - 15A<br>single-phase set $I_{Ph}$ - 10A | 11.5 Nm | 10.48 Nm |
| Dual phase fault<br>$I_{Ph}$ - 15A | 4.8 Nm | 3.5 Nm |

A comparison of torque developed in the healthy, single-phase fault and dual phase fault is shown in Fig. 13. As the sampling frequency of the torque meter is only 100Hz, the double harmonic component in the torque is not visible on the plot. The low frequency torque ripple (approximately 0.1Hz frequency) in the case of dual phase fault is due to weak mechanical coupling in the test setup at low torque values. Theoretically predicted torque values based on the reference currents following (12), (18) and (23) are listed in Table 2.

Transient conditions - speed or load changes are not considered in this work. This work focussed on the current control loops. Speed and load disturbances result in a setpoint change to the current controller. In fault modes, the system gain for the outer speed loop changes as effective torque is lower. This would have implications on achieving speed setpoints. However, within the current limits of the drive converters, the current loop will track the reference and the dynamic performance is demonstrated with the step responses.

## VI. CONCLUSION

In this work, two fault mode control schemes to enable limp home functionality for multi three phase machines are presented. The machine model in ABC domain accounting for inter-winding coupling is used to develop current control scheme capable of fault mode operation. Control structure using PIR controllers are presented. Using the fault mode machine model, it is shown that fault mode controller reconfiguration can be performed with no modifications to controller structure. PIR controllers enable harmonic cancellation similar to VSD control while providing independent controllers per phase. The suitability of PIR controllers for fault modes with single and double open phase fault operation is validated with 3L-NPC inverters.

## ACKNOWLEDGMENT

This work was supported by the INNOVATIVE Doctoral Program, which is funded through the Marie Curie Initial Training Networks action under Grant 665468. This project also received funding from the Clean Sky 2 Joint Undertaking under the European Unions Horizon 2020 research and innovation programme under grant agreement no. 807081.

## REFERENCES

[1] V. Madonna, P. Giangrande, and M. Galea, "Electrical power generation in aircraft: Review, challenges, and opportunities," *IEEE Trans. Transport. Electrific.*, vol. 4, no. 3, pp. 646–659, Sep. 2018.

[2] G. Buticchi, S. Bozhko, M. Liserre, P. Wheeler, and K. Al-Haddad, "On-board microgrids for the more electric aircraft-technology review," *IEEE Trans. Ind. Electron.*, vol. 66, no. 7, pp. 5588–5599, Jul. 2019.

[3] C. Müller, *Opportunities and Challenges of Electric Aircraft Propulsio*, Munich, Germany: Siemens A.G, 2017.

[4] E. Levi, R. Bojoi, F. Profumo, H. A. Toliyat, and S. Williamson, "Multi-phase induction motor drives - A technology status review," *IET Electric Power Appl.*, vol. 1, no. 4, pp. 489–516, 2007.

[5] F. Barrero and M. J. Duran, "Recent advances in the design, modeling, and control of multiphase machines-Part I," *IEEE Trans. Ind. Electron.*, vol. 63, no. 1, pp. 449–458, Jan. 2016.

[6] M. J. Duran and F. Barrero, "Recent advances in the design, modeling, and control of multiphase machines-Part II," *IEEE Trans. Ind. Electron.*, vol. 63, no. 1, pp. 459–468, Jan. 2016.

[7] R. H. Nelson and P. C. Krause, "Induction machine analysis for arbitrary displacement between multiple winding sets," *IEEE Trans. Power Appar. Syst.*, vol. PAS-93, no. 3, pp. 841–848, May 1974.

[8] R. Bojoi, M. Lazzari, F. Profumo, and A. Tenconi, "Digital field-oriented control for dual three-phase induction motor drives," *IEEE Trans. Ind. Appl.*, vol. 39, no. 3, pp. 752–760, May/Jun. 2003.

[9] Y. Zhao and T. A. Lipo, "Space vector PWM control of dual three-phase induction machine using vector space decomposition," *IEEE Trans. Ind. Appl.*, vol. 31, no. 5, pp. 1100–1109, Sep./Oct. 1995.

[10] I. Zoric, M. Jones, and E. Levi, "Arbitrary power sharing among three-phase winding sets of multiphase machines," *IEEE Trans. Ind. Electron.*, vol. 65, no. 2, pp. 1128–1139, Feb. 2018.

[11] J. Karttunen, S. Kallio, P. Peltoniemi, P. Silventoinen, and O. Pyrhönen, "Dual three-phase permanent magnet synchronous machine supplied by two independent voltage source inverters," in *Proc. Int. Symp. Power Electron. Power Electron., Elect. Drives, Automat. Motion*, 2012, pp. 741–747.

[12] Y. Hu, Z. Q. Zhu, and M. Odavic, "Comparison of two-individual current control and vector space decomposition control for dual three-phase PMSM," *IEEE Trans. Ind. Appl.*, vol. 53, no. 5, pp. 4483–4492, Sep./Oct. 2017.

[13] E. Jung, H. Yoo, S. Sul, H. Choi, and Y. Choi, "A nine-phase permanent-magnet motor drive system for an ultrahigh-speed elevator," *IEEE Trans. Ind. Appl.*, vol. 48, no. 3, pp. 987–995, May/Jun. 2012.

[14] A. Galassini, "Distributed speed control for multi-three-phase motors with enhanced power sharing capabilities," Ph.D. dissertation, Power Electronics Mach. Controls Group, Univ. Nottingham, Nottingham, U.K., 2018.

[15] J.-R. Fu and T. A. Lipo, "Disturbance-free operation of a multiphase current-regulated motor drive with an opened phase," *IEEE Trans. Ind. Appl.*, vol. 30, no. 5, pp. 1267–1274, Sep./Oct. 1994.

[16] H. S. Che, M. J. Duran, E. Levi, M. Jones, W. Hew, and N. A. Rahim, "Postfault operation of an asymmetrical six-phase induction machine with single and two isolated neutral points," *IEEE Trans. Power Electron.*, vol. 29, no. 10, pp. 5406–5416, Oct. 2014.

[17] R. R. Errabelli and P. Mutschler, "Fault-tolerant voltage source inverter for permanent magnet drives," *IEEE Trans. Power Electron.*, vol. 27, no. 2, pp. 500–508, Feb. 2012.

[18] B. Li, S. Shi, B. Wang, G. Wang, W. Wang, and D. Xu, "Fault diagnosis and tolerant control of single IGBT open-circuit failure in modular multilevel converters," *IEEE Trans. Power Electron.*, vol. 31, no. 4, pp. 3165–3176, Apr. 2016.

[19] B. R. Lin and T. C. Wei, "Three-phase high power factor rectifier with two NPC legs," *IEE Proc. - Electric Power Appl.*, vol. 150, no. 6, pp. 639–646, 2003.

[20] X. Yuan, W. Merk, H. Stemmler, and J. Allmeling, "Stationary-frame generalized integrators for current control of active power filters with zero steady-state error for current harmonics of concern under unbalanced and distorted operating conditions," *IEEE Trans. Ind. Appl.*, vol. 38, no. 2, pp. 523–532, Mar./Apr. 2002.

[21] F. Rodriguez, E. Bueno, M. Aredes, L. Rolim, F. Neves, and M. Cavalcanti, "Discrete-time implementation of second order generalized integrators for grid converters," in *Proc. 34th Annu. Conf. IEEE Ind. Electron.*, 2008, pp. 176–181.

[22] A. G. Yepes, "Digital resonant current controllers for voltage source converters," Ph.D. dissertation, Dept. Electron. Technol., Univ. Vigo, Vigo, Spain, 2011.

[23] J. Zaragoza, J. Pou, S. Ceballos, E. Robles, C. Jaen, and M. Corbalan, "Voltage-balance compensator for a carrier-based modulation in the

neutral-point-clamped converter," *IEEE Trans. Ind. Electron.*, vol. 56, no. 2, pp. 305–314, Feb. 2009.

[24] J. Wang, X. Yuan, K. J. Dagan, and A. Bloor, "Optimal neutral-point voltage balancing algorithm for three-phase three-level converters with hybrid zero-sequence signal injection and virtual zero-level modulation," *IEEE Trans. Ind. Appl.*, vol. 56, no. 4, pp. 3865–3878, Jul./Aug. 2020.

**JAYAKRISHNAN HARIKUMARAN** received the B.Tech. degree in electronics and communication engineering from the National Institute of Technology Calicut, Calicut, India, in 2008 and the M.S. degree in sustainable energy technology from the Delft University of Technology, Delft, The Netherlands, in 2012.

He has worked in Texas Instruments from 2008 to 2010, Tvilight B.V from 2012 to 2013, and Shell International B.V from 2013 to 2018 on various roles - semiconductor design, embedded systems engineering, industrial control systems and electrical engineering. Since 2018, he has been a Marie-Curie Doctoral Researcher with the Institute for Aerospace Technology, University of Nottingham, United Kingdom. His research interests include design for reliability of power converters, fault tolerant drive systems, and digital controller implementation for power converters in DSP and FPGA.

**GIAMPAOLO BUTICCHI** (Senior Member, IEEE) received the master's degree in electronic engineering and the Ph.D degree in information technologies from the University of Parma, Italy, in 2009 and 2013, respectively. In 2012, he was a Visiting Researcher with The University of Nottingham, U.K. Between 2014 and 2017, he was a Postdoctoral Researcher, and a Guest Professor with the University of Kiel, Germany. In 2017, he was appointed as an Associate Professor of electrical engineering with The University of Nottingham Ningbo China and the Head of power electronics with Nottingham Electrification Center. He was promoted as a Professor in 2020. His research interests include power electronics for renewable energy systems, smart transformer fed micro-grids, and dc grids for the More Electric Aircraft. Dr. Buticchi is one of the advocates for DC distribution systems and multi-port power electronics onboard the future aircraft. During his stay in Germany, he was awarded with the Von Humboldt Post-doctoral Fellowship to carry out research related to fault tolerant topologies of smart transformers.

**MICHAEL GALEA** (Senior Member, IEEE) received the Ph.D. degree in electrical machines design from the University of Nottingham, Nottingham, U.K., in 2013. He was appointed as a Lecturer in 2014, as an Associate Professor in 2018, and as a Professor of electrical machines and drives in 2019 with the University of Nottingham. He currently lectures in Electrical Machines and Drives and in Aerospace Systems Integration and manages a number of diverse projects and programmes related to the more/all electric aircraft, electrified propulsion, and associated fields. His main research interests include design and development of electrical machines and drives (classical and unconventional), reliability and lifetime degradation of electrical machines and the more electric aircraft. He is a Fellow of the Royal Aeronautical Society. He is also an Associate Editor for the IEEE TRANSACTIONS ON INDUSTRIAL ELECTRONICS and *IET Electrical Systems in Transportation*.

**PATRICK WHEELER** (Fellow, IEEE) received the B.Eng. (Hons.) degree from the University of Bristol, U.K., in 1990 and the Ph.D. degree in electrical engineering for his work on Matrix Converters from the University of Bristol, U.K., in 1994. In 1993, he moved to the University of Nottingham, Nottingham, U.K., and was a Research Assistant with the Department of Electrical and Electronic Engineering. In 1996, he became a Lecturer with the Power Electronics, Machines and Control Group, University of Nottingham. Since January 2008, he has been a Full Professor in the same research group. From 2015 to 2018, he was the Head of the Department of Electrical and Electronic Engineering, University of Nottingham. He is currently the Head of the Power Electronics, Machines and Control Research Group, Global Director of the University of Nottingham's Institute of Aerosapce Technology and was the Li Dak Sum Chair Professor in Electrical and Aerospace Engineering. He has authored or coauthored more than 750 academic publications in leading international conferences and journals. He is a Member of the IEEE PELs AdCom and is currently IEEE PELS Vice-President for Technical Operations. He is a Fellow of IET.